REPORT DOCUMENTATION PAGE

Form Approved OMB No. 0704-0188

1. REPORT DATE *(DD-MM-YYYY)*	2. REPORT TYPE	3. DATES COVERED *(From – To)*
09-02-2007	Final Report	1 December 2004 - 01-Apr-07

4. TITLE AND SUBTITLE

Nano-forging of Bulk Metallic Glasses

5a. CONTRACT NUMBER
FA8655-05-M-4077

5b. GRANT NUMBER

5c. PROGRAM ELEMENT NUMBER

6. AUTHOR(S)

Dr. John A Wert

5d. PROJECT NUMBER

5d. TASK NUMBER

5e. WORK UNIT NUMBER

7. PERFORMING ORGANIZATION NAME(S) AND ADDRESS(ES)
Risø National Laboratory
Frederiksborgvej 399
Roskilde 4000
Denmark

8. PERFORMING ORGANIZATION REPORT NUMBER

N/A

9. SPONSORING/MONITORING AGENCY NAME(S) AND ADDRESS(ES)

EOARD
Unit 4515 BOX 14
APO AE 09421

10. SPONSOR/MONITOR'S ACRONYM(S)

11. SPONSOR/MONITOR'S REPORT NUMBER(S)
SPC 04-4077

12. DISTRIBUTION/AVAILABILITY STATEMENT

Approved for public release; distribution is unlimited.

13. SUPPLEMENTARY NOTES

14. ABSTRACT

This report results from a contract tasking Risø National Laboratory as follows: Components with microscale features perform mechanical functions in MEMS devices and store information at the optical (micrometer) scale. Since single-cell microorganisms are on the order of 10 micrometers in size, surfaces with specific topologies on the micrometer size scale have the possibility of topological interactions with such living organisms. Surfaces with nanoscale topological features reduce the size of MEMS devices into the nanoscale regime and have the potential for topological interaction with viruses or large organic molecules.

A manufacturing process to rapidly and cheaply create metal surfaces with topological features in the 10 - 10000 nm scale has not been demonstrated. A potential technique is forging of bulk metallic glasses (BMG). High fidelity replication of topological sine-wave patterns with a periodicity of 800 nm has already been demonstrated at Risø using a BMG of the Mg-Cu-Y type. The advantages of BMG forging are an ability to attain smaller size scales and increased manufacturing speed compared to photolithography, electron beam lithography, and focused ion beam methods. The objectives of the proposed work are to demonstrate the ability to create BMG surfaces with nanoscale surface features, and to establish the capability of existing FEA methods to model BMG flow at these size scales.

15. SUBJECT TERMS
EOARD, Finite Element Methods, MEMS, Microstructure, Nanotechnology, Bulk Metallic Glasses

16. SECURITY CLASSIFICATION OF:			17. LIMITATION OF ABSTRACT	18, NUMBER OF PAGES	19a. NAME OF RESPONSIBLE PERSON
a. REPORT	b. ABSTRACT	c. THIS PAGE			WYNN SANDERS, Maj, USAF
UNCLAS	UNCLAS	UNCLAS	UL	19	**19b. TELEPHONE NUMBER** *(Include area code)* +44 (0)1895 616 007

Final Report

Nano-Forging of Bulk Metallic Glasses

Contract FA8655-04-M4077

Prepared by

John Wert
Materials Research Department
Risø National Laboratory
4000 Roskilde
Denmark
Tlf: +45 4677 5824
john.wert@risoe.dk

September 13, 2006

Table of contents

1. Introduction

Glasses are solids having an atomic scale structure scarcely distinguishable from that of a liquid [1]. Glassy materials fitting the atomic scale structure definition can be found within all material classes: ceramics, polymers and metals. Metallic glasses are the most recently discovered type of glass and their unique characteristics are only starting to be understood and exploited.

The first metallic glass was synthesized at the California Institute of Technology in 1960 by Klement, Willens and Duwez [2]. Splat cooling was used to rapidly cool an $Au_{75}Si_{25}$ alloy from the molten state and subsequent X-ray diffraction revealed diffuse peaks characteristic of an amorphous atomic arrangement. From 1960 until the 1980s, rapid cooling was thought to be essential for synthesis of metallic glasses. The situation changed markedly in 1990 when Inoue and co-workers announced synthesis of a metallic alloy that remained amorphous at slower cooling rates [3,4]. Inoue's discovery showed that several rare-earth-containing alloys, for example La-Al-Ni, could be fabricated into fully amorphous rods with diameters of several millimetres by casting the alloy into a copper mould. While Inoue is widely credited with the discovery of metallic glasses that could be produced in bulk form, his discovery was the endnote of a series of earlier research projects by Chen [5] and by Turnbull et al. [6,7], each of which demonstrated an increase in the diameter of a fully amorphous metallic alloy rod compared to earlier known results. Alloy compositions that can be synthesized as glasses in thicker sections are normally referred to as *Bulk Metallic Glasses* (BMG) to distinguish them from metallic glasses that require rapid cooling.

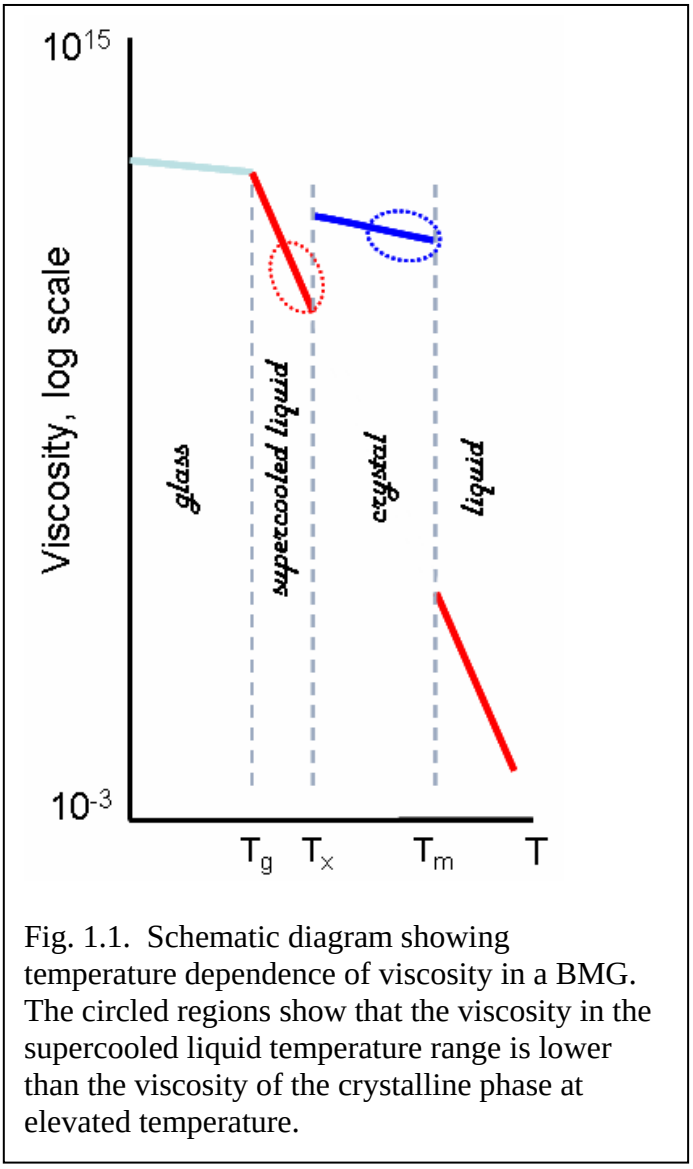

Fig. 1.1. Schematic diagram showing temperature dependence of viscosity in a BMG. The circled regions show that the viscosity in the supercooled liquid temperature range is lower than the viscosity of the crystalline phase at elevated temperature.

Normally, the division between rapidly cooled metallic glasses and BMG is identified as a critical cooling rate of 10^3 K/s [8]. For metallic glasses with critical cooling rates lower than about 10^3 K/s, the crystallization temperature, T_x, is higher than the glass transition temperature, T_g, and the glass transforms to a supercooled liquid state before crystallizing, Fig. 1.1. In contrast, metallic glasses with

critical cooling rates higher than 10^3 K/s exhibit T_x below T_g. This means that rapidly cooled metallic glasses have so little resistance to crystallization that even the modest atomic mobility below T_g is enough to allow crystallization. This shows that the difference between rapidly cooled metallic glasses and BMG is more significant than arbitrary specification of a critical cooling rate: BMG persist as amorphous materials in a supercooled liquid state above T_g whereas rapidly cooled metallic glasses do not.

Transformation of BMG into a supercooled liquid state at the glass transition temperature is an exceptional characteristic, as illustrated in Fig. 1.1. This schematic diagram shows that the resistance to deformation (= viscosity^{-1}) drops dramatically at T_g, attaining values (red dotted circle) substantially below those attained by crystalline metals, even when heated near their melting temperatures (blue dotted circle). The low viscosity translates into a remarkable ability to shape BMGs in the supercooled liquid state.

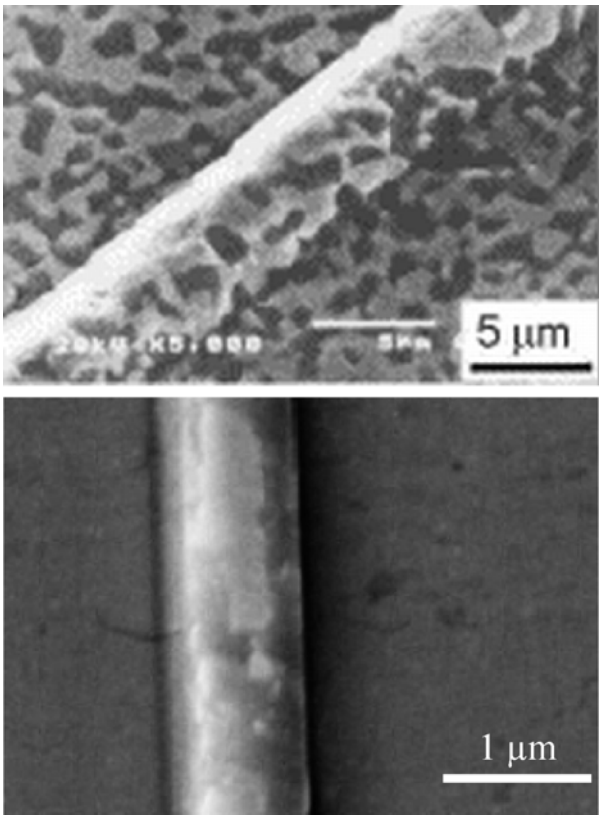

Fig. 1.2 Comparison of the fidelity of BMG surface replication on a fine scale. The upper figure is from an article by Saotome et al. [9].

Crystalline metallic materials usually undergo deformation processing at elevated temperatures to take advantage of lower flow stress and higher ductility. However, elevated temperature deformation activates microscopic mechanisms, such as grain boundary sliding, that give rise to inhomogeneous deformation. As a consequence, surface unevenness develops on the scale of the grain size during hot working processes. For large components

the surface roughness is usually negligible, but for small components the grain-scale surface roughness can be sufficient to interfere with their function. Forming parts from BMG completely avoids this problem because there are no microstructural structural features larger than the nanometer scale.

Fig. 1.2 illustrates the difference in surface quality obtained in a shaping process with crystalline and amorphous metals. The upper micrograph shows the result of a forming process using a superplastic Zn-Al alloy with a grain size near 1 μm. The surface roughness associated with individual grains is apparent. The lower figure demonstrates that the surface produced by forming of a Mg-based BMG in the supercooled liquid temperature regime. In this case, the small surface roughness is attributable mainly to fragments of oxide that were present on the BMG surface before deformation (whitish patches on top of the raised ridge) rather than to the grain size or other microstructural feature size.

This example demonstrates that fabrication of components with intricate shapes or fine scale surface features is possible using BMG. While BMG show much promise for fabrication of micro- and nano-scale devices, only a few demonstration components have been reported with micrometer scale features and virtually no systematic studies of features with over a broad size scale range have carried out. The present study was undertaken to explore opportunities for shaping of micro- and nano-scale components using bulk metallic glasses, and to create the beginning for a systematic understanding of the phenomena involved in such shaping operations.

The goal of work during the present period is twofold.

- Demonstrate the capability to create features substantially smaller than 100 nm by imprinting of BMG surfaces.
- Compile a short description of potential applications for such capabilities.

2. Synopsis of Results from Previous Interim Contract Report

In the previous contract period, a Si imprinting die containing various patterns was fabricated. The patterns were a set of 3 lines with widths of 1000, 500 and 100 nm, and several shallow logos. A BMG of composition $Mg_{60}Cu_{30}Y_{10}$ was imprinted using this die. The imprinting conditions were 50 MPa for 5 minutes at 167ºC. This BMG has a T_g of 145ºC and can be held for about 30 minutes at 170ºC before evidence of crystallization can be detected by X-ray diffraction. Thus, the imprinting conditions were designed to maintain the amorphous condition of the alloy.

The imprinted surface was examined using SEM imaging. The upper part of Fig. 2.1 shows the die prior to imprinting and the lower part shows the imprinted BMG surface, both at the location of the 3 lines. The lines correspond to depressions in the die, and raised ridges on the imprinted BMG surface.

A quantitative analysis of the imprinted BMG surface was carried out to determine the height of the imprinted ridges. The results were plotted as (ridge height) vs. (groove width); earlier data for grooves ranging from 150 to 750 μm in width was included. A linear relationship was obtained on a log-log plot, which was interpreted a demonstrating that the

friction between the BMG and the die, as well as surface tension of the BMG, had little influence on the imprinting process in the size range from 100 nm to 1 mm.

Extrapolation of the results to smaller groove widths is possible. But the influence of surface tension and/or friction could become significant or other unexpected factors could perturb the imprinting process. Thus, a goal of pushing the imprinting process to features smaller than 100 nm was selected.

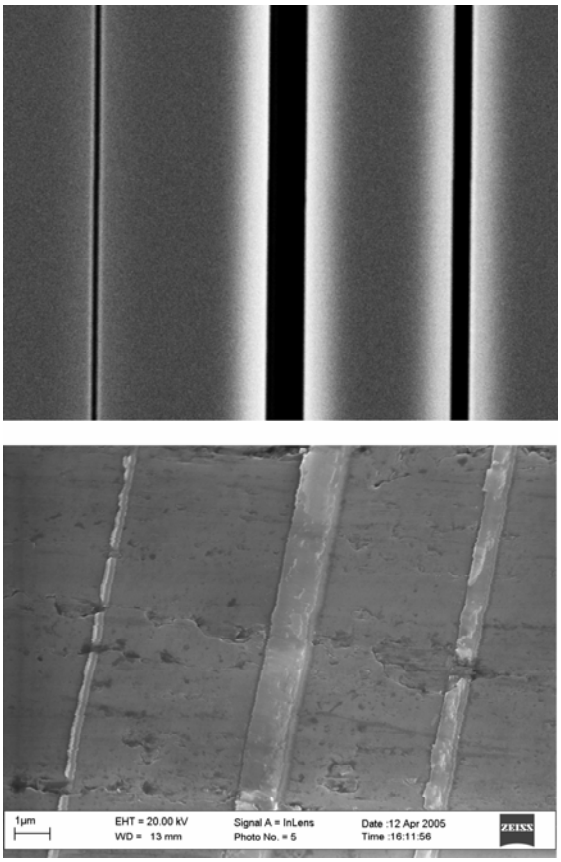

Fig. 2.1 The die (upper) and imprinted BMG(lower) at the position of the 3 linear features.

3. Demonstration of Imprinting of Features < 100 nm

Imprinting Dies

Making an imprinting die by FIB processes is time consuming and the precision of the FIB etching process may be limited for feature sizes extending downward from 100 nm toward 10 nm. The uncertainty over the quality of results obtained with the FIB die making process, combined with the long time required, led to development of an alternate method for making dies with sub-100 nm features. While this method is inexact, it is suitable for initial trials.

The method developed employed stainless steel die blocks which were mechanically polished to a final mirror finish. These blocks were 8 mm x 8 mm, with a thickness of 2

mm. Observation of the die blocks after the polishing procedure revealed no linear features that could be confused with features later intentionally introduced.

To create the imprinting features, grit particles were blended with lapping oil. Three different suspensions were prepared: using grit particle sizes of 1000 nm, 250 nm and 50 nm. These were standard zirconia grinding media. To prepare linear features on a stainless steel die, one drop of one of the suspensions was placed on a carefully cleaned silica glass plate. A stainless steel blank was then placed face down on the plate, and was translated about 5 mm using moderate downward pressure. The process was repeated with each of the suspensions. Microscope observations after this die preparation process revealed arrays of linear features, in the orientation corresponding to the translation direction, and of size corresponding to what would be expected from the process employed.

BMG Material

The BMG used for imprinting was that used previously: $Mg_{60}Cu_{30}Y_{10}$. This material was melted under a protective Ar atmosphere and gravity cast into a Cu mold with dimensions 25 mm x 25 mm x 2.2 mm thick. Several castings, totaling about 50 g were prepared. The slabs were then sectioned into rectangular test pieces, measuring 5 mm x 5 mm. The test pieces were mechanically polished to a 0.05 μm finish about 2 hours before imprinting.

Some aspects of the Mg-Cu-Y alloy are attractive for the imprinting operations carried out in the present study. It has a relatively low T_g temperature, 145ºC, which means that deformation experiments can be carried out in the temperature range 165-170ºC. This low imprinting/forging temperature is valuable for two reasons:

- the die does not need to be made of high temperature material
- oxidation of the BMG prior to imprinting is not excessive

The latter point may be of some significance for imprinting at the nanoscale. As indicated in connection with Fig. 1.2, the oxide film present on the surface of the BMG is fragmented in places where the surface is “stretched” during imprinting. The areas between the oxide fragments have a thinner oxide layer than the areas where the original oxide layer fragments remain. The presence of the original oxide fragments is the main factor contributing to roughness of the imprinted surface.

Imprinting Method

In the previous experiments, imprinting was performed using a miniature closed forging die. The present experiments were conducted using gas pressurization. The principle of this process is shown in Fig. 3.1.

i. The substrate is heated to the imprinting temperature, 170 ºC.
ii. The die and BMG are placed on the substrate, and a thin aluminium membrane is placed on top of the die + BMG.
iii. The upper part of the pressurization chamber then closes, creating a gas-tight seal around the periphery of the aluminium membrane.
iv. A heating period of 5 minutes is allowed to ensure that the die + BMG were at the desired temperature.
v. The upper chamber is pressurized to 7 MPa, the maximum pressure obtainable with this machine.

vi. The pressure is maintained for a period of 10 minutes.
vii. The pressure is released and the die + BMG were removed and cooled.

One difference between the earlier experiments with a die prepared by FIB methods and the present method was the lower pressure obtainable in the present experiment: 7 MPa vs 50 MPa.

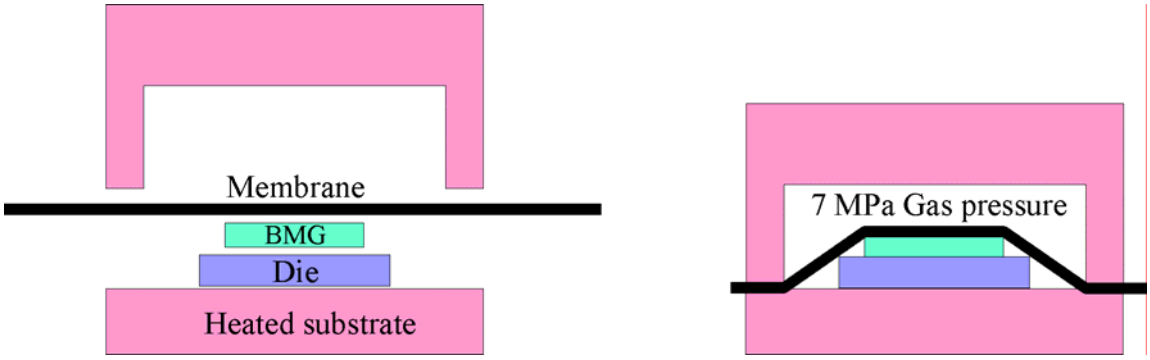

Fig. 3.1 Gas pressure imprinting equipment used in the present study.

A second difference is that the gas-pressure operated press is located in a class 1000 clean room at Risø. Using equipment in a clean room presents both advantages and disadvantages. Advantages include reduced dust contamination of the imprinted BMG. Disadvantages include difficulty of access to the equipment (training course is required to work in the clean room facility), inability to mechanically polish the oxide layer off of the BMG within a few seconds prior to placing it in contact with the die, and limited pressure available for imprinting.

The present imprinting experiments were the first to be performed in the clean room facility. There are several trade-offs involved. The trade-off between oxide build up in the several-hour period between polishing and imprinting vs. the reduction in dust contamination was unknown. The present results show that oxidation prior to imprinting layer is a more severe problem than dust, for the $Mg_{60}Cu_{30}Y_{10}$ BMG composition used here. There is also a trade-off in terms of the effort involved in working in a clean room facility. Working in the clean room is generally cumbersome, but the gas-operated press is largely automatic and simpler to use than a furnace mounted on a hydraulic testing machine.

Imprinting Results

Due to lack of access to an AFM for measuring the imprinted surface within a short period after the imprinting process, only qualitative results are available in the form of SEM micrographs of the imprinted surfaces.

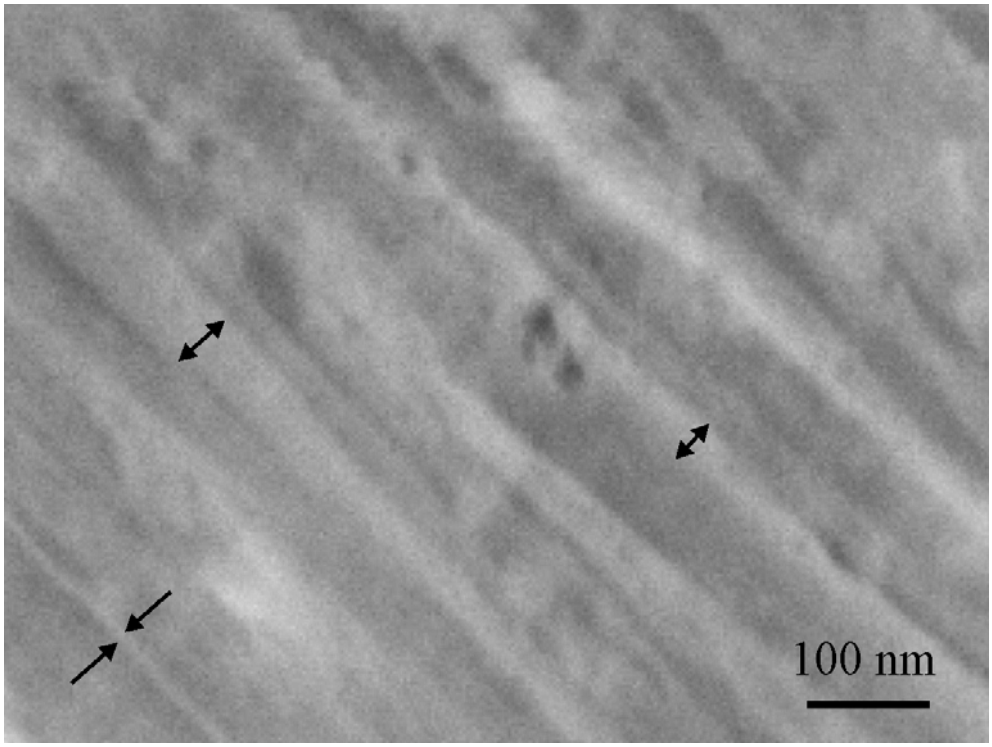

Fig. 3.2 Imprinted BMG using die made with 1000 nm zirconia powder. Arrows indicate the width of ridges on the BMG surface.

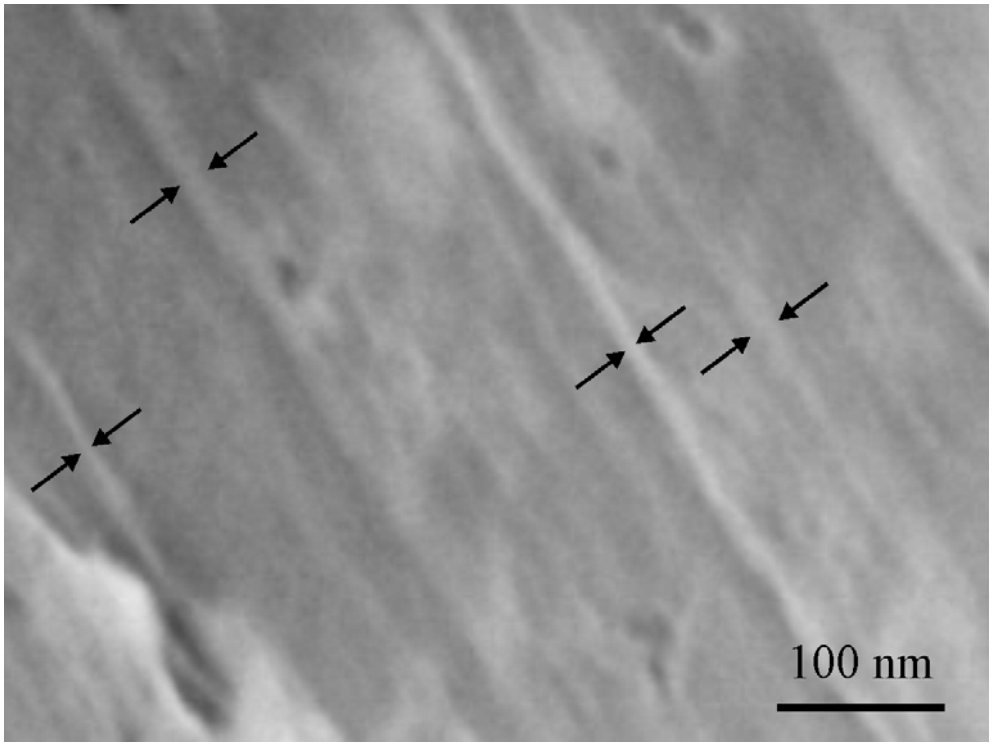

Fig. 3.3 Imprinted BMG using die made with 250 nm zirconia powder.

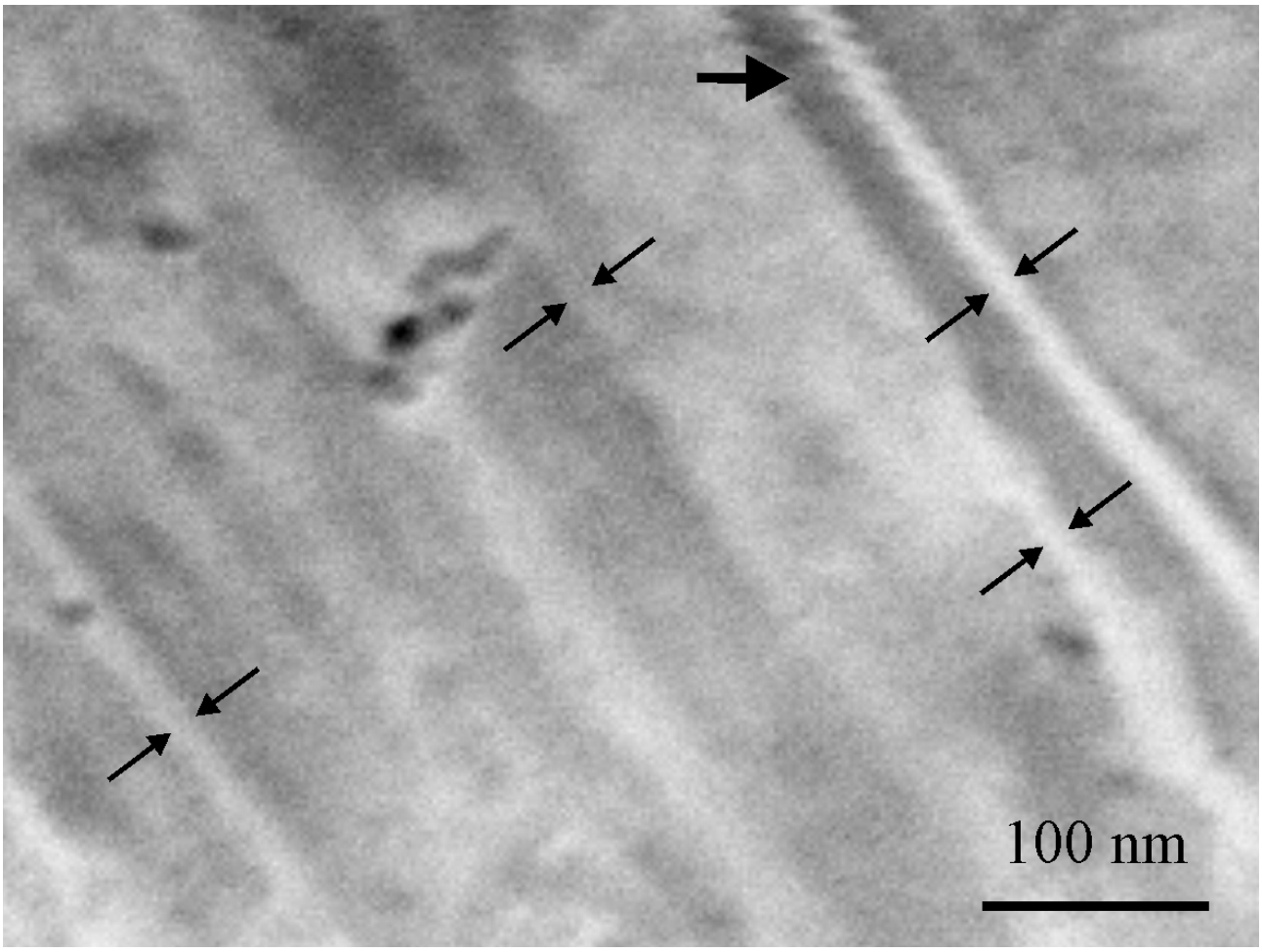

Fig. 3.4 Imprinted BMG using die made with 50 nm zirconia powder.

On each of the imprinted BMG surfaces, linear features corresponding to the direction of the scratch marks on the dies were located. These were successfully imaged in an SEM at high magnifications, 40kX – 100kX using very small working distances (2 – 3 mm). Tilting of the samples, which was previously used to measure ridge height after imprinting, was not possible using the short working distances required for these observations. Mechanical vibrations were a significant disturbance for observations at this magnifications – the effect of such vibrations can be clearly seen at the top of Fig. 3.4 (single arrow), originally taken at 80kX.

Table 3.1 Measurements of the typical width of raised features on the BMG surfaces, as a function of the grit size used to create the dies.

Grit size used to create the die, nm	Typical feature width on the imprinted BMG, nm
1000	30
250	20
50	12

By the time the AFM was available for use, the surfaces made by imprinting had oxidized and were no longer of use for detailed measurements. However, results in Table 3.1 indicate that the widths of the ridges observed on the BMG surfaces correlate with the size of grit used to create the stainless steel dies. This provides evidence that the SEM observations are not artifacts of patterns on the stainless steel or on the BMG sample pieces, but are a product of the imprinting process.

The smallest imprinted features imaged in the present study are about 50 atoms wide. The effect of surface tension on shaping of nanoscale surfaces has often been questioned. In the present case, the imprinting pressure was released before the BMG cooled below T_g. If surface tension had a significant effect on the imprinting process, it would have been expected to smooth the surface in the interval after imprinting and before cooling below T_g. The fact that ridges were observed on the imprinted surface indicates that this did not happen to a substantial degree, at least for ridges larger than 10 nm in width. This observation is consistent with the fact that imprinting parameters similar to those used for imprinting of larger features, also worked with features down to 10 nm. If factors such as surface tension were significant for imprinting of 10 nm features, extra pressure would have been required to overcome the surface tension, rather than the lower pressure actually used.

This result conflicts with an earlier report by Saotome et al. [10] who suggested a surface tension effect during forming of features as large as 1 μm using a Pd-based BMG. It seems possible that there are large enough variations in surface tension among BMG of various compositions to account for the different interpretations, but observations available at the present time are insufficient to clarify this discrepancy.

While the results are unfortunately qualitative, the observations allow the following conclusions.

- Imprinting of linear features having widths down to 10 nm has been demonstrated.
- Evidence suggests that factors such as surface tension do not such have such a large influence at the 10 nm scale that they dominate the imprinting process.

4. Outlook for Micro/Nano- Forming of BMGs

Which BMG are best for micro/nano-imprinting?

When a BMG is heated into the temperature range above T_g, it is in a liquid state. The liquid is not free-flowing, but the rheological behaviour is that of a high viscosity liquid. For such materials, the apparent viscosity – the ratio of flow stress and strain rate – determines the progress of shaping operations, such as imprinting. Thus, it is appropriate to consider whether there are strong differences in the viscosity among various BMG families, differences sufficient to influence the performance of BMG in imprinting operations.

The flow stress –strain rate relationship for BMG is of type

$$\sigma \propto \dot{\varepsilon} \qquad (4.1)$$

For axisymmetric stress –strain rate tests, the viscosity (η) is defined as

$$\eta = \frac{\sigma}{3\dot{\varepsilon}} \tag{4.2}$$

the factor of 3 arising when shear strain rate is converted to uniaxial strain rate and shear stress is converted to uniaxial stress.

At higher strain rates, the relationship is of power law type:

$$\sigma \propto \dot{\varepsilon}^{n} \tag{4.3}$$

Kawamura [11] and Spaepen [12] have proposed constitutive relations for the two regimes. FEM simulations with the two formulations yield essentially identical results. The constitutive formulation shown here is the Kawamura formulation.

$$\eta = B \exp\left(\frac{H}{RT}\right)\left[1 - \exp\left(\frac{D}{\left\{\dot{\varepsilon} C \exp\left(H^{*}/RT\right)\right\}^{\beta}}\right)\right] \tag{4.4}$$

The factors B, H, D, C, H* and β are material constants, and R is the gas constant.

Using data published in the literature, the 6 material constants appearing in the constitutive equation have been determined for 3 BMG compositions. Table 4.1 lists these values.

Table 4.1. Material parameters for viscosity relation

Alloy composition	*B* Pa s	*H* KJ/mol	*C* s	*H** KJ/mol	*D*	β	T_f °C	$\eta(T_f)$ Pa s
$Mg_{60}Cu_{30}Y_{10}$	5×10^{-24}	274	7×10^{-29}	230	-0.05	0.4	170	1×10^{9}
$Zr_{65}Al_{10}Ni_{10}Cu_{15}$	8.4×10^{-19}	363	3.1×10^{-21}	261	-0.0049	0.84	410	5×10^{9}
$Pd_{40}Ni_{40}P_{20}$	2.4×10^{-42}	580	7.0×10^{-26}	278	-0.012	0.82	235	2×10^{8}

By algebraic manipulation, Eq (1) and (2) can be written:

$$\dot{\varepsilon} = \sigma\left[\frac{1}{3B}\exp\left(-H/RT\right)\right] + \left\{\sigma\left[\frac{-C^{\beta}}{3BD}\exp\left(\frac{BH^{*} - H}{RT}\right)\right]\right\}^{\frac{1}{1-\beta}} \tag{4.5}$$

Using this relation and the values in Table 4.1, the strain rate as a function of flow stress and temperature can be calculated for each of these BMG.

In the previous analysis, the viscosity at the crystallization temperature T_x was calculated and used as a basis for comparison. While scientifically meaningful, virtually no time is available for shaping at T_x, prior to the onset of crystallization. A better comparison would be at a forming temperature T_g and T_x – labelled T_f – where sufficient time is available for a shaping operation.

Table 4.1 shows the result for T_f 30º above T_g, a temperature typically used for forming processes. The table shows that viscosity at this temperature increases in the order $Pd_{40}Ni_{40}P_{20}$, $Mg_{60}Cu_{30}Y_{10}$, $Zr_{65}Al_{10}Ni_{10}Cu_{15}$. This suggests that, while the Zr-based BMG has many excellent properties, easy formability is not among them. To form the Zr-based BMG at the same rate as the Pd-based BMG listed in Table 4.1, the applied stress needs to be about 25x higher and the forming temperature is over 400ºC instead of 235ºC for $Pd_{40}Ni_{40}P_{20}$ and 170 ºC for $Mg_{60}Cu_{30}Y_{10}$. The resulting pressure and temperature requirements for the forming die are much more demanding for the $Zr_{65}Al_{10}Ni_{10}Cu_{15}$ BMG. This is thought to be a major factor accounting for the observation that there are far fewer articles describing microforming of Zr-based BMG than Pd-based and Mg-based BMG.

Comparing these results for BMG with traditional silica glass technology, it is found that the viscosity of silica glasses is much lower than that of BMGs at practical forming temperatures. The softening point for silica glasses is defined as the temperature corresponding to a viscosity of 4×10^8 Pa s and the working point is defined as the temperature corresponding to a viscosity of 1×10^5 Pa s. The BMG compositions that have been discovered thus far do not attain viscosities below about 10^6 Pa s even at the crystallization temperature where essentially no time is available for shaping.

The difference can be explained by the higher resistance to thermally induced crystallization of silica glasses compared to BMG. For typical silica glasses the working temperature is 400 or 500ºC higher than T_g, and silica glasses can be held in the working temperature range for considerable periods without crystallization. For BMG, the crystallization temperature is rarely more than 100 ºC above T_g. Thus, the BMG that are known today cannot be shaped as readily as silica glasses, but they have a substantially lower viscosity in the supercooled liquid temperature regime than traditional crystalline materials even near the melting temperature. These considerations indicate that forming processes for BMG are not identical to either those used for making silica glass components or those used for shaping traditional crystalline metal components.

Does BMG preparation method matter?

It should be noted that the flow characteristics described above do not apply to marginal glass forming alloys – metallic glasses that require high cooling rates to retain the amorphous structure during cooling. Such materials, which have a lower resistance to crystallization than bulk metallic glasses, crystallize before reaching T_g. When marginal glass forming alloys are heated, they crystallize before transforming to a supercooled liquid; thus they never exhibit the rheological characteristics of a supercooled liquid. Equation (4.4) does not apply to such materials.

Note that the key factor is the relationship between T_g and T_x. A bulk metallic glass has $T_g < T_x$, whether it is prepared by conventional casting or melt spinning. The above material

model applies to materials with $T_g < T_x$, regardless of the method used to prepare them. Thin ribbons of bulk metallic glass compositions are equally amenable to the imprinting process as thicker pieces prepared by more conventional casting operations.

Properties of BMG below T_g

A variety of reviews have been published describing service properties of BMG. While BMG have notably high hardness and (compression) yield strength, they do not exhibit significant plastic extension in tension. This is generally understood to be a consequence of propagation of shear for the first shear band to form. In constrained loading conditions, such as bending, hardness indentation and near notch tips, multiple shear banding has been reported in some specific BMG compositions. The effect is to spread plastic flow over a larger volume of material. In such constrained loading conditions, BMG exhibit better plastic flow properties than silica glasses, for example. However, no cases of substantial ductility have been reported for monolithic BMG subject to pure tensile loading.

For traditional engineering applications, the lack of ductility in pure tension is an important limitation. However, this appears to be less of a factor for many microscale components. There are two reasons for this.

1. Tensile ductility below T_g is not required for shaping operations, those can be carried out above T_g. Furthermore, the requirements for microcomponents generally focus on a few specific properties required for the component's function, rather than optimization of a suite of engineering properties. For example, microcomponents used as electrical contact springs in miniature electronic devices must be electrical conductors, must have high enough fatigue resistance so the spring can operate reliably over a period of years, and must be resistant to specific corrosive environments. But tensile ductility is not a service requirement. Similarly, microcomponents that make up MEMS devices must meet various specific property requirements, but the "bend-before-break" standard applied to engineering materials appears to be of lesser importance for at least some microscale components.

2. Thin strips of BMG appear to have significantly greater bend ductility that thicker pieces of material. This is apparently related to the greater density of shear bands developed in thinner pieces, although a convincing physical explanation of this effect remains elusive. Since imprinted patterns at the microscale can be created on substrates of virtually any thickness, the possibility exists to take advantage of this scale-dependent bend ductility effect, if needed.

In the present study, the goal is to explore the opportunity for imprinting micro and nanoscale patterns on BMG surfaces. Such devices could be used for a variety of applications, as listed in the following section. For many of these applications, tensile ductility is not a requirement. This argument indicates that, as a general rule, reducing the scale of a component and increasing the specificity of its function reduces the number of critical material properties.

Opportunities

The opportunity exists to make surface patterns having a lateral scale in the range 10 nm to 1 mm, and a depth scale similar to the lateral scale. The starting materials must be a BMG, with a thickness at least twice the depth of the surface patterns. This means that for surface patterns with depths less than about 20 µm, melt spun ribbon with a thickness on the order of 50 µm is a suitable starting material. For patterns with greater depth, a casting method producing a thicker material is required. The die can be any material that can withstand the temperature and pressure of imprinting. In experiments carried out so far, sticking of the BMG workpiece to the die has not been encountered.

What could such imprinted metallic surfaces be used for?

The following list contains various general ideas for such applications. References are provided in conjunction with some of the ideas.

Trapping of fluids in surface depressions.

It is possible that trapping of a fluid in the depressions when two surfaces are brought into contact could be of use in some cases [13]. If the fluid is a lubricant, the surface depressions would serve as distributed lubricant reservoirs between two sliding surfaces.

There may be other applications where trapping of fluids in micro-scale pockets on a surface would be beneficial. These could include medical applications where an analgesic or antibiotic drug in fluid form could be trapped in pockets on the surface of a medical instrument. When the instrument is used, the fluid would be brought into direct, immediate contact with surfaces. If the instrument is a cutting blade, for example, the freshly cut surfaces could be in contact with the fluid after motion of as little as a few micrometers. [No published information about such applications was found.]

Diffraction

Surfaces with periodic patterns at the 500 nm scale have uses as diffraction gratings for radiation at optical wavelengths. Optical holograms shaped from plastic appear on standard consumer items and, with lower quality, on packaging. Dies for such holograms are currently made by photolithography of Si followed by Ni plating. Optical gratings of various complexity have been made at Risø by imprinting BMG with Ni dies.

The potential exists to make smaller patterns that would be useful with shorter wavelength UV radiation. Plane focussing monochromators suited to wavelengths below 100 nm, for example, have potential uses in semiconductor processing and high-density holographic information storage. Such devices have the possibility to operate at sub-optical wavelengths where conventional optical elements are inefficient or fail because they lose transparency for the incident radiation.

The methods demonstrated so far are suitable for manufacturing gratings/holograms throughout the UV range: near-UV (200 – 300 nm wavelength), far-UV (91 – 200 nm) and longer extreme-UV wavelengths (10 – 91 nm). It is conceivable that optical elements for

longer wavelength X-rays could be fabricated in the same way, although the feature size would need to be in the 10 nm range. This capability has been demonstrated in the current work.

Nanofeatured surfaces in medical devices

Studies of interaction of biological tissue with surfaces having topological features at the nanoscale are rather common. In the biomedical field, these are often called nanofeatured surfaces.

One broad area of research involves attachment of cells from a larger organism onto nanofeatured surfaces. As a research topic, this area appears to be rather well developed and potential technological applications are quite near, or may already be in place. The idea is that growth and migration of cells can be influenced by the topology of surfaces they are in contact with. A simple example involves implants with nanofeatured surfaces that promote cell attachement – with the goal of improving integration of the implant into the body. The effects are well established and rather positive results can be achieved, but it appears that manufacturing nanofeatured surfaces over large areas of irregularly shaped objects is a major limitation. This appears to be an area in which imprinted BMG surfaces could have a major impact. The limitation is the rather narrow span of BMG compositions, many of which contain elements unsuitable for medical implants in humans. Zr- and Ti- based BMG may be favourable in this respect, but rigorous biocompatibility studies have apparently not been done for any BMG. Pd- and Pt based BMG may also be useful in some limited circumstances, but the cost of such implants might be a limiting factor.

A second concept involves growth of cells on nanofeatured surfaces for the purpose of generating a damaged network structure. Curtis [14] summarized studies in which networks of neurons were grown on a surface, containing nanoscale patterns designed to encourage nerve cell interconnections of the type found in natural nervous systems. In some cases, the nanofeatures were chemical patterns, in other cases the patterns were topological. Merz and Fromhertz [15] demonstrated growth of stable networks of neurons on a microfabricated surface containing pits and grooves. The feature sizes were on the order of 20 to 100 μm in this study. The surface was created on a polyester layer on a Si substrate using conventional lithography techniques. If a suitable die was available, fabrication of BMG surfaces, which could be subsequently coated with a thin insulating film by any of several deposition processes if necessary, could be done rapidly.

Topological surface features that match individual micro and nanoscale objects

In addition to surfaces that interact with cells in an organism, there is the possibility of creating nanofeatured surfaces with a topology at a smaller scale that interacts with bacteria, viruses, bacteriophages, organic molecules, etc. Bacteria are generally in the size range 1 – 10 μm and have shapes ranging from simple elongated ellipsoids to more complex spirals. The topological shapes of bacteria are known from optical microscopy, but the shapes are also known to depend on the environmental conditions. Viruses and bacteriophages are smaller (roughly in the size range 50 to 500 nm). The topological shapes have in a few cases been revealed by TEM tomography [16]. Large organic molecules can have a wide variety

of forms, ranging from chains as in linear polymers to rings and stars in either 2D or 3D; the molecular size can be a few nm up to µm.

In all of these cases, there is the possibility to create surfaces with a topology that interacts with the organism/molecule. One could envision that the organism/molecule would be attracted to the patterned surface by either a pure topological interaction, by a chemo-topological interaction promoted by deposition of a chemical layer on the topologically patterned surface, or by application of an external field. The nanofeatured surface would then prompt the organisms/molecules to arrange in a pattern on the surface. This could be for the purpose of studying interactions between the organisms/molecules, promoting reactions between them, or detecting their presence or absence in the environment in which they were immersed.

At present, only scattered information is available on these topics. For example, Dalby et al. [17] reported that fibroblasts (type of cell found in connective tissue) responded differently to two types of nanofeatured surfaces. These researchers emphasized that study of the interaction between cells and nanofeatured surfaces is an exciting topic, but they cited two limitations in such studies. One is that the mechanisms of such interactions are almost completely unknown. The second is the extreme cost and difficult of producing the nanofeatured surfaces (their study used e-beam lithography). It would appear that the ability to produce 10's or 100's of square cm of nanofeatured surfaces from a single die, would be a benefit to such studies. The current project demonstrated that this ability exists with BMG, down to a feature size scale of 10 nm.

Forming of MEMS components

The potential for fabricating micro or nanoscale components for MEMS/NEMS applications is obvious and results from demonstration projects have been published. Imprinting of sprockets has been a popular demonstration topic, as well as ridges of various shapes. However, going beyond the concept of creating components for MEMS devices by shaping BMG in the supercooled liquid regime to components used in actual devices seems difficult. No published reports of components incorporated into a functional device could be found, although shapes on surfaces that could be of use as elements in MEMS devices have been reported [for example: 9,10,18]. The Japanese group led by Y. Saotome, which published much of the initial work on the micro-forming topic in the period 2000-2002, has published virtually nothing on this topic since 2004.

A second characteristic of this topic is the poor state of development of processing science. The relatively few articles written on this topic draw mainly on knowledge of shaping processes related to thermomechanical processing of bulk crystalline metallic materials. The behaviour of viscous liquids, corresponding to the actual state of the BMG being shaped, is distinct from creep of polycrystalline metals. An appreciation of the unique limitations and capabilities of shaping BMG components depends on improved understanding of the processing science of these materials

Although evolution of BMG microcomponents is not occurring rapidly, that should not interpreted as a lack of opportunity. The author of this report is part of a join Danish government – Danish industry project to develop prototype BMG microcomponents having

size scales in the range 100 μm to 1 mm. Based on this experience, the main challenge is not development of BMG materials. The challenge is educating design engineers, product engineers and toolmakers about the possibilities of using BMG materials to manufacture products that are not feasible to make with conventional metals.

5. Conclusions

1. Imprinting on the surface of a BMG of linear features having widths down to 10 nm has been demonstrated.

2. Evidence suggests that factors such as surface tension do not such have such a large influence at the 10 nm scale that they dominate the imprinting process with Mg-based BMG.

3. A variety of applications exist for surface patterns with feature sizes in the sub micrometer scale. These have yet to be exploited to any significant extent. One reason is that the opportunity to create metal surfaces covered with nano – micro-scale features, at a rate of perhaps 1 m^2 / hour, is not generally understood.

6. Reference List

1. Angell CA, Science **267**;1995:1924.
2. Klement W, Willens RH, Duwez P, Nature **187**;1960:869.
3. Inoue A, Zhang T, Masumoto T, Materials Trans JIM **30**;1989:965.
4. Inoue A, Yamaguchi H, Zhang T and Masumoto T, Materials Trans JIM, **31**;1990:104.
5. Chen HS, Acta metal. **22**;1974:1505.
6. Drehman, AL, Greer AL, Turnbull D, Appl. Phys. Letters, **41**;1982:716.
7. Kui HW, Greer AL, Turnbull D, Appl. Phys. Letters, **45**;1984:615.
8. Inoue A, Acta mater. **48**;2000:279.
9. Saotome Y, Miwa S, Zhang T, Inoue A, J. Materials Provessing Technology, **113** (2001) 64-69.
10. Saotome Y, Imai K, Shioda S, Shimizu S, Zhang T, Inoue A, intermetallics, 10 (2002) 1241-1247.
11. Kawamura Y, Nakamura T, Kato H, Mano H, Inoue A, Mat. Sci. Eng. **A304-306** (2001) 674-678.
12. Spaepen F, Scripta materialia, **54** (2006) 363-367.
13. Shimizu I. Andreasen JL, Bech J, Bay N, J. Tribology, **123** (2001) 290-294.
14. Curtis A, Nature, **416** (2002) 274-275.
15. Merz M, Fromherz P, Adv. mater. **14** (2002) 141-144.
16. Jiang W, Chang J, Jakana J, Weigele P, King J, Chiu W, Nature 439, 2006, 612-616.
17. Dalby, MJ, Riehle, MO, Sutherland, DS, Agheli H, Curtis, ASG, Euro J Cell Biology, **83** (2004) 159-169.
18. 17. Saotome Y, Iwazaki, J Materials Processing Technology, 119 (2001) 307-311.